Effect of the Acoustic Impedance in Ultrasonic Emitter Transducers using Digital Modulations

M. S. Martins[a,b,*], J. Cabral[a], S. Lanceros-Mendez [c] and G. Rocha[a]

[a]Minho University, Algoritmi Center

[b]Instituto Politécnico do Cávado e do Ave, Departamento de Tecnologias

[c]Center/Department of Physics, University of Minho, Campus de Gualtar, 4710-057 Braga, Portugal

Abstract: In an underwater environment it is difficult to implement solutions for wireless communications. The existing technologies using electromagnetic waves or lasers are not very efficient due to the large attenuation in the aquatic environment. Ultrasound reveals a lower attenuation, and thus has been used in underwater long-distance communications. The much slower speed of acoustic propagation in water (about 1500 m/s) compared with that of electromagnetic and optical waves, is another limiting factor for efficient communication and networking. For high data-rates and real-time applications it is necessary to use frequencies in the MHz range, allowing communication distances of hundreds of meters with a delay of milliseconds. To achieve this goal, it is necessary to develop ultrasound transducers able to work at high frequencies and wideband, with suitable responses to digital modulations. This work shows how the acoustic impedance influences the performance of an ultrasonic emitter transducer when digital modulations are used and operating at frequencies between 100 kHz and 1 MHz. The study includes a Finite Element Method (FEM) and a MATLAB/Simulink simulation with an experimental validation to evaluate two types of piezoelectric materials: one based on ceramics (high acoustic impedance) with a resonance design and the other based in polymer (low acoustic impedance) designed to optimize the performance when digital modulations are used. The transducers performance for Binary Amplitude Shift Keying (BASK), On-Off Keying (OOK), Binary Phase Shift Keying (BPSK) and Binary Frequency Shift Keying (BFSK) modulations with a 1 MHz carrier at 125 kbps baud rate are compared.

Keywords: Underwater Acoustic Channel, Underwater Wireless Communication, Transducer Optimization, Piezoelectric Ultrasound Emitter Transducers, Digital Modulations.

1. Introduction

The oceans still hide a large potential in areas such as pharmaceutics, oil, minerals and biodiversity, but the difficulty in communicating in this environment makes ocean exploration a tremendously challenging task. The existing Radio Frequency (RF) technologies are difficult to use in this environment and therefore, there are many research efforts to develop reliable wireless underwater communication technologies (Che et al. 2010). One of the technologies that has shown to be very promising, due to the low attenuation, is Ultrasounds (Sameer et al. 2012; Stojanovic & Preisig et al. 2009). Although ultrasounds show a low propagation speed of approximately 1500 m/s, the delay can be acceptable for real-time communications at distances up to some hundred meters, since to tens of kilometers the propagation delay can reach a few seconds, disabling real-time communications. The subaquatic channel also reveals other significant challenges that influence the development of underwater acoustic communication systems, such as attenuation, which increases with frequency, ambient noise, Doppler Effect, and time-varying multipath.

To develop high data-rate wireless communication systems in underwater environments it is important to incorporate the state of the art of conventional digital modulation techniques. Therefore, there are several projects under development (Chitre et al. 2008; Preisig et al. 2006; Martins et al. 2014), such as the work presented by Kim et al. 2010 which presents an underwater communication system with modulations as Amplitude Shift Keying (ASK), Binary Frequency Shift Keying (BFSK), Quadrature Phase Shift Keying (QPSK) and 16 Quadrature Amplitude Modulation (16QAM) to transmit an image over a distance of 15 m, reaching a bit-rate of 3 kbps with carriers from 17 kHz to 23 kHz. Another project is the commercial

*Corresponding author. Tel.:+351 253 510180; fax:+351 253 510189.
E-mail address: mmartins@dei.uminho.pt (M. Martins).

product presented by EvoLogics et al. 2013, with different underwater acoustic modem models, with a maximum data rate of 31.2 kbps, with a frequency band from 48 kHz to 78 kHz. The project described by Nowsheen et al. 2010 presents a high data-rate underwater acoustic modem FPGA based, where it was implemented a BPSK modulation with 800 kHz carrier, reaching 80 kbps rate.

Nonetheless, ultrasound communication systems are still very limited, with very low data rates and high delays, mostly due to the physical characteristics of the subaquatic channel. Using carriers with upper frequencies, the attenuation increases leading to a decrease of the distance reached. For a 1 MHz signal, the acoustic absorption achieves 280 dB/km and to this effect also the spreading attenuation has to be added, which depends on the transducer geometry.

Ultrasound transducers are usually manufactured with piezoelectric materials and, to maximize the output pressure level with low consumption, the transducer must operate at the resonance frequency as described by Sherman & Butler et al. 2007.

There are several factors that influence the signal quality: structural damping, electrical damping and acoustic impedance mismatch. Structural damping is due to the energy dissipation in geometrical deformations of the transducer when the electrical field is applied. Electrical damping is due to transducer capacitor effects which result in a time lag between the application of the electrical signal and the transducer response. However, to the 1 MHz limit range, the most significant factor is the acoustic impedance mismatch, since the structural and electrical damping only affects the signal quality above tens of MHz in piezoelectric ceramic transducers and hundreds of MHz in piezoelectric polymer transducers (M. S. Martins et al. 2010). The acoustic impedance mismatch, between the transducer and the medium, causes acoustic waves to be reflected back to transducer. The resonance transducers are designed to overcome this fact, since the internal acoustic waves are synchronized with the electrical drive signal, causing an addition of the two signals and therefore increasing the output. On the other hand, to communicate using digital modulations it is not advisable to operate with resonance transducers since synchronization is not possible due to the lack of periodicity of the modulated signal.

This work is focused in the study of the influence of the acoustic impedance on the ultrasonic transducer performance, operating with high and wideband frequencies (100 kHz to 1 MHz range), using digital modulations, being also addressed how to improve the signal quality.

The projector used in this study was a piston type with a piezoelectric disk, which operates in the thickness mode. The piston-type transducer was selected because it is easy to be manufactured and is low-cost. The study presented in this work is not exclusive for the transducers under consideration and it can be applied to other types of piezoelectric transducers, since the study just shows the interference of the acoustic signals when the energy is transferred from the transducer to the medium. Two types of piezoelectric materials were used: the ceramic Lead Zirconate Titanate (PZT) (high acoustic impedance) (Bove et al. 2001) and the polymer Polyvinylidenefluoride (PVDF) (low acoustic impedance) (Wang et al. 2006; Sencadas et al. 2009).

With the objective of evaluating the performance of ultrasound transducers using digital modulations, such as: Phase-Shift Keying (PSK), Frequency Shift keying (FSK) and Amplitude Shift Keying (ASK). A Matlab/Simulink Model was developed to estimate the transducer performance to guide transducer construction and performance evaluation, since it allows for the most suitable design to be selected. Using Field Programmable Gate Arrays (FPGAs), a reconfigurable platform to develop all the necessary building blocks to implement different types of digital modulations was developed. Two experimental set-ups were developed: a small water tank, where digital modulations measurements were carried out to perform signal analysis and to validate the simulation model; and a swimming pool where the difference of linearity of both types of piezoelectric materials were studied for a wide frequency range.

1.1 Piezoelectric transducers background

This section introduces the main concepts on piezoelectric transducers needed to support the decisions made in the materials selection and transducer dimensioning and fabrication.

Usually, at high frequencies piezoelectric ultrasonic transducers operate in the 33 mode, that is, the deformation is along the polarization axis and the excitation electric field point in the same direction. The free displacement of the material in direction 3, without restraining force and assuming uniform strain over the surface, according Leo et al. 2007 is given by:

$$\xi = d_{33} v$$

Eq.1

where ξ is the free displacement, v is the applied voltage and d_{33} is the coupling coefficient in the thickness direction. The deformation creates a pressure wave in the medium, whose force amplitude can be obtained according to Sherman & Butler et al. 2007, by:

$$F = pA_p,\ p = 2\pi c \rho f \xi$$

Eq.2

where c is the sound speed, ρ is the material density, A_p is the area of the piezoelectric element and f is the signal wave frequency.
In order to increase the pressure wave amplitude, several piezoelectric disks, in a stack configuration, can be used. This configuration allows multiplying the free displacement by the number of layers n. In this case, the displacement is given by (Abrar & Cochran et al. 2004):

$$\xi = d_{33} v n$$

Eq.3

Despite this increase in strain, the intensity of the produced force does not change (Leo et al. 2007; Lewin & Bloomfield et al. 1997). The maximum force that the piezoelectric element can apply to a medium is obtained by:

$$F = d_{33} \frac{A_p}{S_{33}^E t_p} v$$

Eq.4

where S^E_{33} is the elastic compliance coefficient and t_p is the thickness of a single layer.

To ensure good acoustic signal quality, the force that the transducer can apply to the medium must be greater than the generated acoustic wave force, otherwise, the piezoelectric material displacement will be deformed, generating acoustic waves with low amplitude and noise. This condition allows for the calculation of the layer thickness and the number of layers for a specific frequency and material. Through equations 2 and 4 it is possible to obtain:

$$n t_p \leq \frac{1}{2\pi c \rho S_{33}^E f}$$

Eq. 5

Another important aspect is related to the transducer acoustic impedance. The sound wave created inside the transducer reflects, in part, at the boundary established by different densities ρ and bulk modulus B of

the transducers and the medium. This reflection creates deformations on the acoustic signal transmitted to the medium, which can be calculated by:

$$S_{out}(t) = T_w\left(S_{in}(t) + LR_wS_{in}(t + D_p)\right)$$

Eq.6

Here, S_{out} and S_{in} are the output sound wave and the sound wave created inside the active element, respectively, in Pascal (Pa) as function of time (t), T_w is the transmitted sound wave intensity percentage, R_w is the reflected sound wave intensity percentage, L is the internal energy loss and D_p is the delay of the reflected sound wave, introduced by the active element thickness.

2 Materials Selection and Transducer Fabrication

Before carrying out the experimental validation, piezoelectric materials and transducer dimensions needed to be selected. This section will describe the materials selection and the transducer manufacture.

Among all the piezoelectric materials, the most common to these types of applications are the ceramics: Lead Zirconate Titanate (PZT), Lead Titanate (PT), Lead Magnesium Niobate (PMN) and Lead Zinc Niobate (PZN) (Abrar & Cochran 2004; Bove et al. 2001; Shrout et al. 2008). However, other often used materials are the polymers Polyviylidenefluoride (PVDF) and P(VDF-TrFE) (Levassort et al. 1998; Schmerr et al. 2006; Shrout et al. 2008; Lewin & Bloomfield et al. 1997) and single crystals of PZT, PMN and PZN (Saitoh et al. 1998; Yamamoto et al. 2013).

This study focuses on PZT-5H since this is the most interesting material for large scale applications due to its availability and price. For comparison, the PVDF polymer will be used, since it is an interesting material due to the low acoustic impedance ($3.3x10^6$ kg/m²s) and price. With values near to the medium acoustic impedance ($.5x10^6$ kg/m²s), it is possible to minimize the acoustic signal distortions and allow a better acoustic energy transference from the transducer to the medium, resulting in a reduction of the acoustic energy accumulated inside the transducer.

For a better understanding on how the acoustic impedance mismatch influences the ultrasonic transducer performance, Figure 1 shows the acoustic pressure wave along the transducer thickness and the medium, when positioned at the center of the acoustic pattern. The transducer dimensions were defined to operate at 1 MHz resonance frequency, resulting in a 2.05 mm thickness for PZT-5H and 1.125 mm for PVDF, and a diameter with 2.5 times the wavelengths.

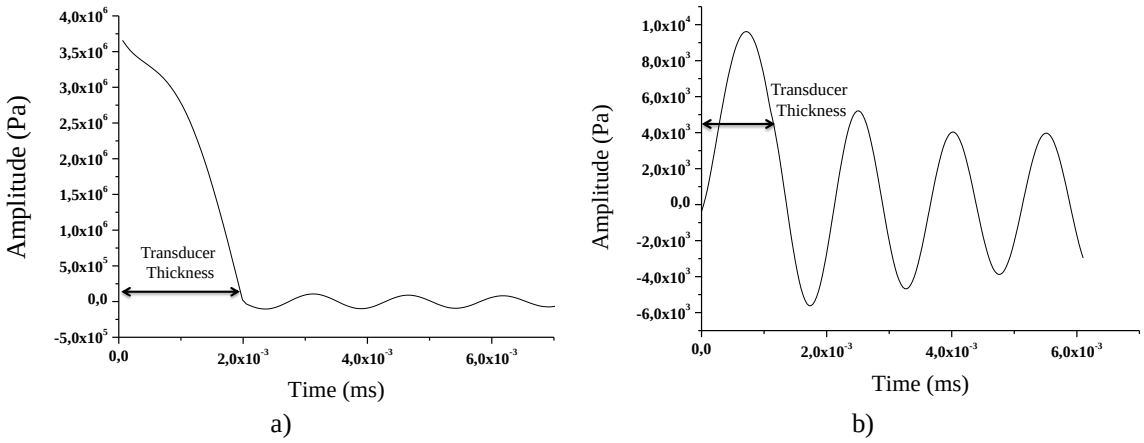

Figure 1: FEM simulation of two piston transducers: PZT-5H (a) and PVDF (b).

Figure 1a shows that the pressure wave inside the PZT-5H transducer has a much higher level than the acoustic pressure transferred to the medium, since the boundary between the two materials holds back

most of the acoustic energy. In Figure 1b this effect is reduced, with the acoustic energy having a better transference form the transducer to the medium.

The utilization of a matching layer, in this case, would not be useful since the frequency of the digital modulation signal would be unknown leading to unknown matching layer thickness. With electronic control it is possible to improve the signals quality by overcoming the internal energy, but this means high power consumption and cost.

These signals were obtained from a FEM simulations using a multiphysics platform in a 2D symmetric plane considering piezoelectric strain models for the active element actuation and pressure acoustic model for the pressure waves. The simulations setups are the same for all transducers, where only the active element is replaced. The outside boundaries of the medium were configured as *match boundaries* to work as absorbers, removing all the echoes. The selected *mesh* is divided in areas with triangular shape and a size of 10% of the wavelength. The simulations were performed with the following settings: fresh water as propagation medium, 20 C° of temperature and sine wave excitation signal with 12 V of amplitude.

Further, the results will be representative for their respective family of materials: ceramic, polymer and piezoelectric, respectively.

The transducer design specifications must be exclusive for each material, ensuring the best performance. The PZT-5H transducer dimensions were defined to operate at the resonance frequency to replicate the conventional commercial transducers. Else, the PVDF transducer dimensions were defined to operate at the optimal conditions for 1 MHz range, generating non periodic signals.

Before defining the transducer dimensions, it is necessary to verify if the piezoelectric material has the required strength to produce vibrations at 1 MHz frequency in underwater environments. Table A.1 shows the main physical properties and the project considerations of these materials for the proposed application, according to equations 1 to 6:

Table A.1: Comparison of some characteristics of PZT-5H and PVDF (M. Martins et al. 2012).

Physical Property	PZT-5H 2mm	PVDF 8x28
Thickness(m)	2,00E-3	2,80E-5
Resonance Frequency (Hz)	1,05E+6	5,02E+6
Sound Speed (m/s)	4,20E+3	2,25E+3
Density (kg/m^3)	7,50E+3	1,47E+3
Acoustic Impedance *Z* [10^6kg/m²s]	33	3.3075
Relative Dielectricic constant Ɛr	3100	12
Piezoelectric Coefficient d_{33} (C/N)	5,12E-10	3,40E-11
Elastic compliance coefficient S_{33}^{E} (1/Pa)	2,07E-11	4,72E-10
Layers	1	8
Max Applied Force/Excitation Tension (N/V)	3,88	8,08E-1
Applied Force at 1MHz/Excitation Tension (N/V)	1,49	7.92E-1
Max Operating Frequency Underwater (Hz)	2,61E+6	1,02E+6
Transmitted wave percentage at 1MHz (%)	32%	78%

In order to operate at 1 MHz resonance frequency, the PZT-5H disk must have a thickness of 2 mm.

From Table A.1, PZT-5H shows that a larger force than the necessary can be applied to the medium without sacrifice the piezoelectric material full displacement. However, PVDF has a higher S^{E}_{33} than

PZT-5H, and therefore it cannot be applied the displacement to the medium at the same vibration frequencies with the same material thickness.

Therefore, the solution for the lack of force and for the acoustic energy retained inside the active element is the use of thin films. From equation 4, by reducing the active element thickness, it is possible to increase the force applied to the medium and, by equation 6, reducing the active element thickness results in a decrease of the internal reflected wave propagation delay. This will minimize the signal distortion since the transmitted and reflected waves will be almost synchronized.

For the PVDF, a multilayer topology to increase the acoustic performance (Abrar & Cochran et al. 2004; Martins et al. 2012) was selected and, at 1 MHz operational frequency, the thickness of the PVDF transducer was limited by the piezoelectric strength (Eq.6). In this case, the total thickness could not exceed 225 µm. According to Martins et al. 2012, a PZT transducer shows an acoustic pressure output 21.9 dB higher than the one for PVDF. However, using a structure of 8 layers of 28 µm thick PVDF, it is possible to reduce this difference to 5.5 dB. With 225 µm the PVDF transducer has a resonance frequency of 5 MHz, but in an underwater environment it just shows the necessary strength to reach 1 MHz.

The eight layers of the transducer were then glued with silicone in a compression press. Finally, the active element was glued to a stainless steel mass and the active element outside surface was isolated with a thin silicone layer to protect it from water. Each layer was connected with a parallel drive excitation circuit. As the number of layers increases the performance is improved, but manufacturing complexity and power consumption also increases.

Therefore, the multilayer transducer was manufactured. In Martins et al. 2012 it is possible to find more details about the assembling methods used in transducers described above.

3 Simulations and Experimental Setup

3.1 Sceneries Setup

The swimming pool dimensions are: 12 m long, 4 m wide and 3m deep. Two test distances were defined: 10 cm and 12 m, where measurements were performed at 50 cm deep and in the middle of the pool (2 m either side). It was used fresh water at a temperature of 13 ºC and 7.2 pH. The drive signal was a sine wave of 100 cycles burst with 16 V amplitude and at each distance, several frequencies were measured: 100 kHz, 200 kHz, 300 kHz, 400 kHz, 500 kHz, 600 kHz, 700 kHz, 800 kHz, 900 kHz, 1 MHz, 1.2 MHz and 1.4 MHz.

The second scenario used for the digital modulations evaluation, both in real tests and simulations, was a small water tank with 120×50×40 centimeters (length, width, height). The ultrasonic transmitter and receptor position coordinates were (22.5; 23; 11) and (87.5; 23; 11) centimeters. With these dimensions, echoes occur very easily and therefore a matching boundary (foam) at the boundary in front of the projector was used. The foam did not completely eliminate all the echoes but it was still possible to ensure the same settings for the two transducers tested.

Different tests with different modulations were performed: ASK, FSK and PSK were selected. All the modulations were defined as binary with just 1 bit per symbol. Accordingly, two types of modulations were defined from the ASK, BASK and OOK.
Figure 2 shows the drive signals used in both simulations and real experiments.

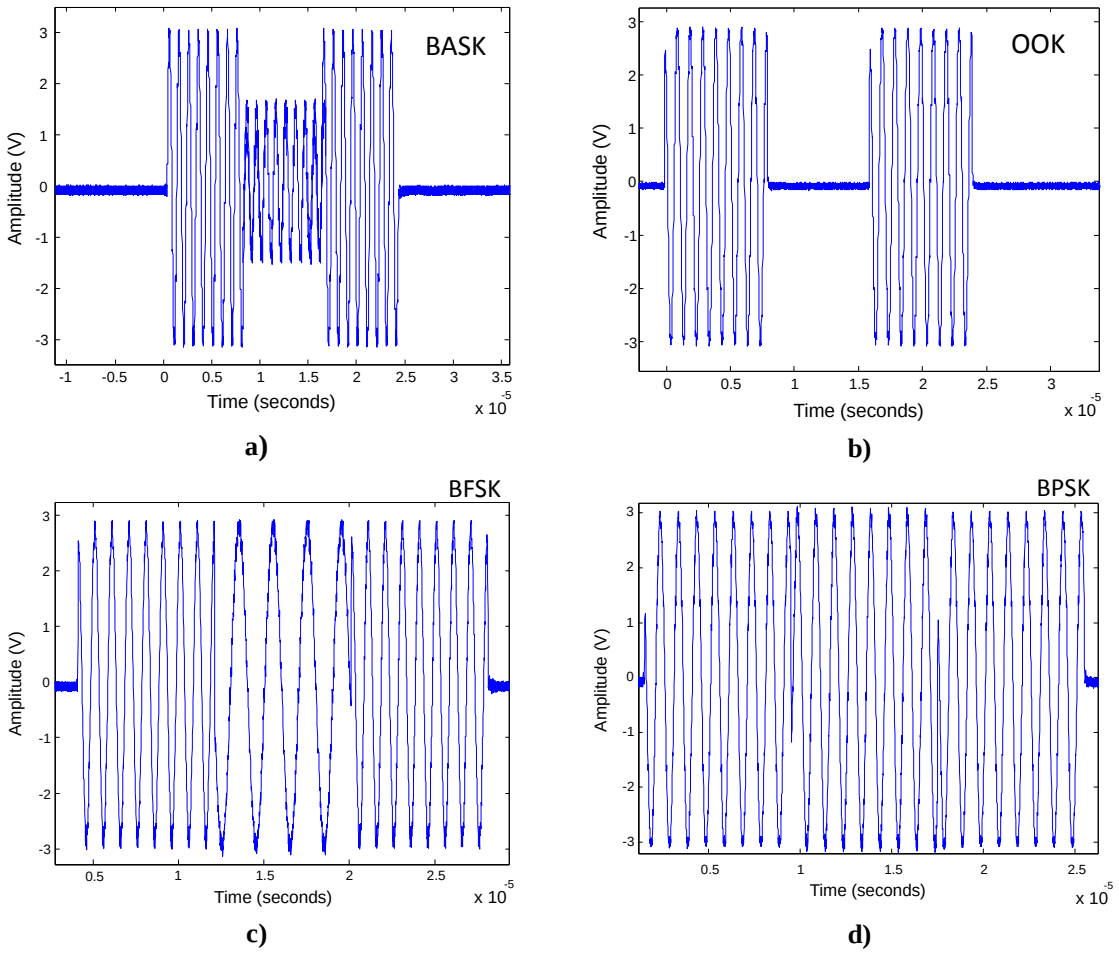

Figure 2: Drive signal of digital modulations, a) BASK, b) OOK, c) BFSK and d) BPSK.

Figures 2a, 2b, 2c and 2d display the drive signals at the transmission module output for BASK, OOK, BFSK and BPSK, respectively. The signals were generated at 25 Mega samples per second with 14 bit. Since the highest carrier has a frequency of 1 MHz, it is possible to ensure a very good signal quality with 25 samples per period. Before being sent to the transducer, these signals were amplified 4 times, resulting in a 12 V excitation voltage. High variations of frequency and phase were applied for the BFSK and BPSK in order to allow an unbiased analysis of the transducer performance in the worst case scenario. In this sense, no correction or external interference, like filters or equalizers, was used.

In the BASK modulation (Figure 2a), the low logic level was set to half of the high logic level amplitude, and in OOK (Figure 2b) the high level was the same as BASK, but with no signal at the low level. In the BFSK (Figure 2c) the high logic level was set to 1 MHz and the low logic level to 500 kHz. This high difference between frequencies allows for an easy analysis of the results, since close frequencies would be masked by the resonance effect. But this difference will be limited by the Doppler Effect and it will depend on the underwater environmental conditions, since it is necessary to ensure that the Doppler shift does not exceed the difference between the frequencies of different levels. In the BPSK modulation (Figure 2d) the logic level transition is made by a 180º phase shift.

The bit stream selected for tests was a sequence of ‘101’, being therefore possible to analyze the transducer reactions to a ‘0’ to ‘1’ and ‘1’ to ‘0’ transitions. The bit period selected for these tests was 8 µs, corresponding to 8 cycles at 1MHz. For a better understanding of this decision, Figure 3 shows the PZT-5H transducer response for a signal burst with 4, 8 and 16 µs periods.

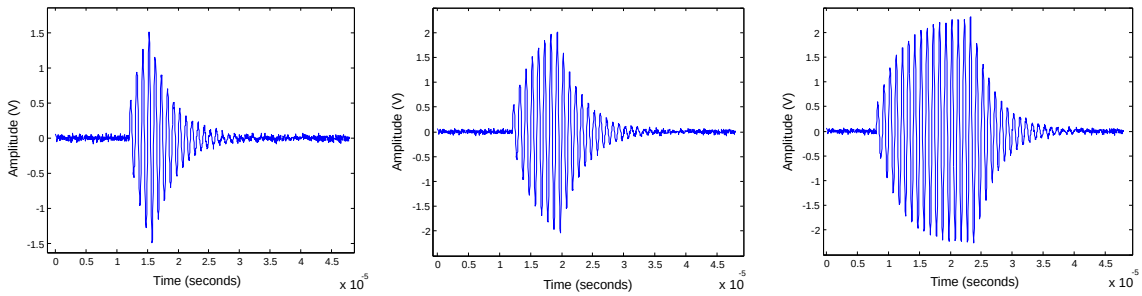

Figure 3: PZT-5H transducer response for a signal burst with 4, 8 and 16 µs periods at 1 MHz.

Figure 3 shows that the minimum time necessary for the signal start to stabilize is around 8 µs. Then, to increase the probability of sending a good quality signal, it was decided not to use bit periods much below 8 µs. With 8 µs bit period and 1 MHz carrier, the baud rate is 125 kbps.

3.2 Simulations

A Matlab/Simulink model was developed to simulate the ultrasonic transducers performance for different piezoelectric materials. The Simulink block was defined with 8 inputs and 1 output. The inputs are the excitation electrical signal, the water acoustic impedance and the piezoelectric material proprieties: density, sound speed, piezoelectric coefficient, elastic compliance coefficient, thickness and the number of layers. The output is the acoustic wave signal generated by the transducer. The block diagram presented in Figure 4 represents a simplified view of the model and helps to understand the relationships between the different sub-blocks.

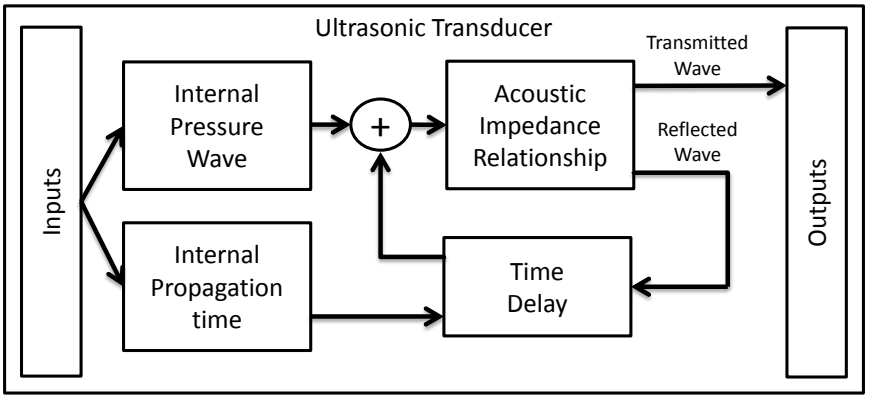

Figure 4 - Block diagram of the MatLab/Simulink simulation.

The block diagram is based on equation 6. The model begins by calculating the pressure wave generated inside the transducer and it is calculated using a transfer function, where it is included frequency proportionality with a zero based in equation 2. It also were included two poles for the electrical and structural damping, according to Leo et al. 2007. Based on the transducer acoustic impedances and on the medium parameters, the transmitted and reflected pressure wave amplitudes are calculated. The reflected wave suffers a time delay, corresponding to the internal propagation time and, in a closed loop system it is added to the current internal pressure wave. The model was implemented as a discrete model with a sampling time of 40 ns, corresponding to a frequency sample of 25 Mega samples per second.

3.3 Experimental test system

In order to evaluate the results of the subaquatic channel model, experiments were carried out in a test tank. The system configuration is shown in Figure 5.

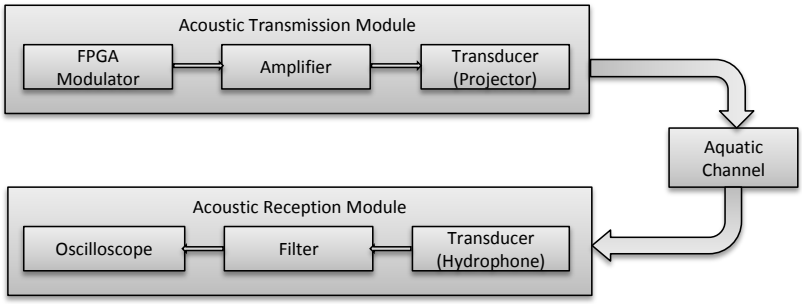

Figure 5 - Block diagram of the test system.

The acoustic transmitter module is made up of a Xilinx Spartan-3A FPGA starter kit that it is responsible for modulating a bit stream into an electrical signal. Then the drive signals from the FPGA modulator are amplified by a 5 W Classe B Push-Pull symmetric voltage amplifier with a maximum gain of 12 dB.

The ultrasonic receptor used to register the pressure waves was the Cetacean ResearchTM C304XR hydrophone, with a transducer sensibility of -201 dB, re 1 V/µPa and a linear Frequency Range (±3dB) of 0.012–1000 kHz. The filter consists of a 2nd order active band-pass from 1 to 2000 kHz with 6 dB gain. The digital oscilloscope used to record the measurements was a PicoScope 4227 100 MHz. Both PZT and PVDF piston type emitting transducers were homemade: the PZT transduces has a 2 mm thickness and 2 cm diameter and the PVDF one has a 8 x 28 µm multilayer structure with 2 cm diameter.

4 Results and Discussion

As was referred before, two materials types were evaluated: PVDF and PZT-5H. The results include an analysis of the frequency range linearity and the digital modulation performance.

4.1 Frequency Range response

Figure 6 shows the amplitude response of the two transducers over a wide range of frequencies: 100 kHz to 1.4MHz to different distances: 10 cm (Figure 6a) and 12 m (Figure 6b).

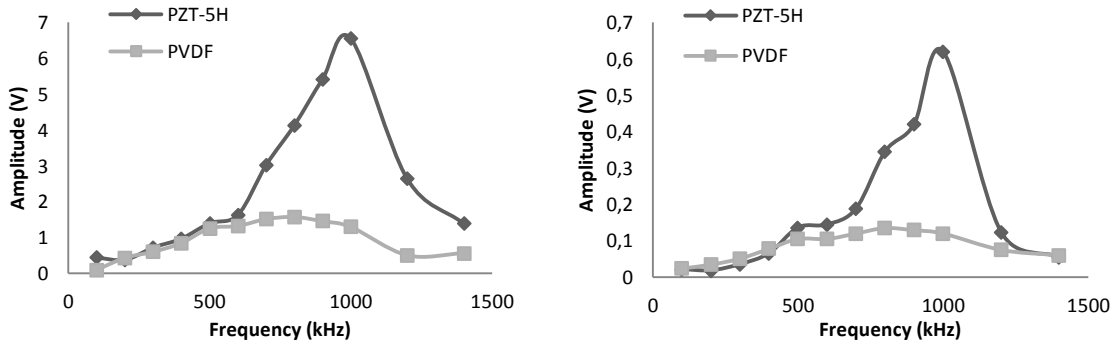

a) b)

Figure 6: Transducer acoustic pressure response from 100 kHz to 1 MHz, for 10 cm (a) and 12 m (b) distance.

It is observed that PZT-5H has a higher acoustic pressure output, but the response is not linear, with the highest level at resonance frequency point of 1 MHz. Both materials in Figure 6 show an acoustic output with a growing tendency between 100 kHz and 1 MHz. At 10 cm (Figure 6a) the PZT-5H displays a

growth of 13.7 dB between 100 kHz and 500 kHz, but if the range between 500 kHz and 1 MHz was considered the growth reaches 16.6 dB. Conversely, the PVDF displays a growth of 14.8 dB between 100 kHz and 500 kHz range, but to a frequency range between 500 kHz and 1 MHz only reach 3.6 dB.

In Figure 6b, results for a 12 m distance shows the same tendency: the PZT-5H displays a growth of 16.2 dB between 100 kHz and 500 kHz and 19.6 dB between 500 kHz and 1 MHz. The PVDF has a lower growth: 7.4 dB to the first interval and 3.7 dB to the second interval.

In conclusion, PZT shows a better response in terms of acoustic power. On the other hand, with respect to the bandwidth, PVDF displays an almost flat response between 500 kHz and 1 MHz, this flat behavior meeting the requirements for digital communications with high data rates.

4.2 Digital Modulations

The two materials were simulated and measured with real tests for 4 modulation types: BASK, OOK, BFSK and BPSK.

Figure 7 represents the PZT-5H transducer responses to the BASK and OOK amplitude modulations, respectively.

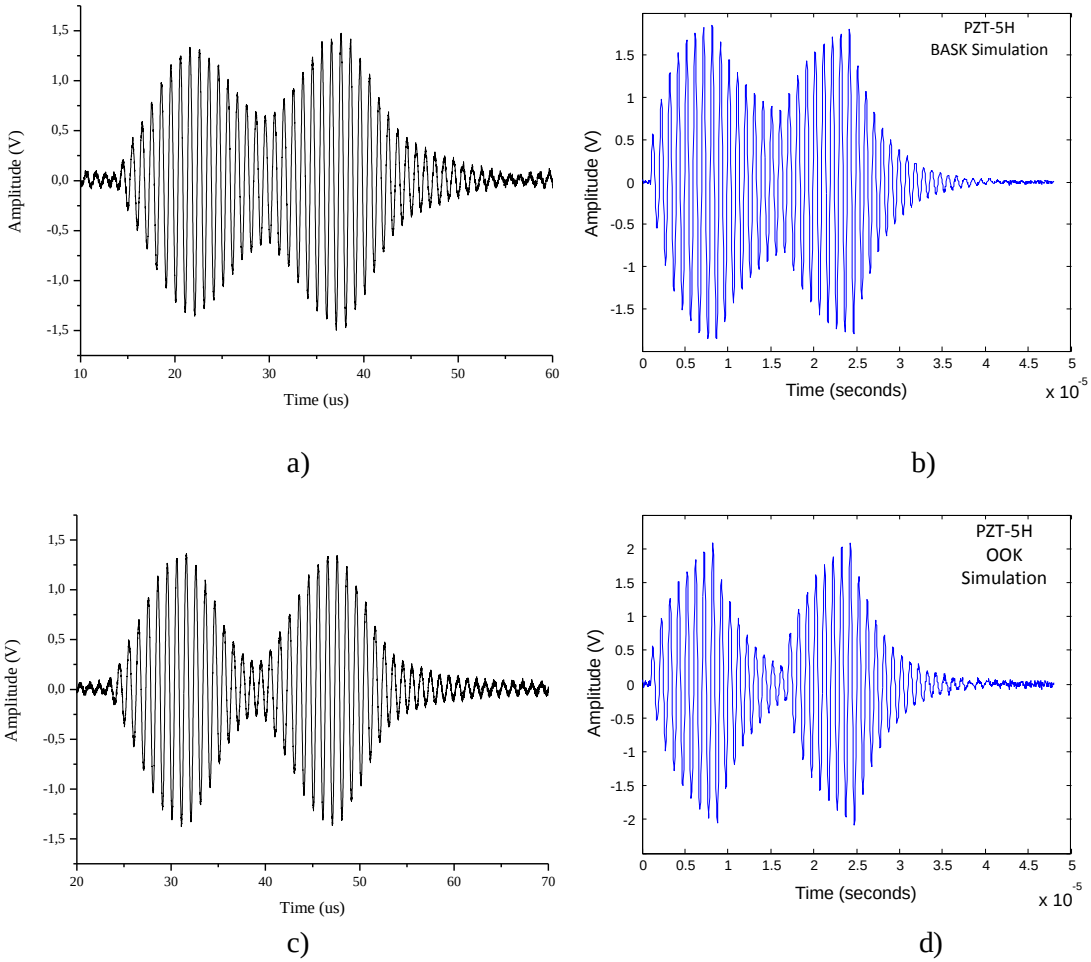

Figure 7: PZT-5H response to BASK and OOK modulations, real measurement and simulation.

In both amplitude modulations, the results are very similar, being only a difference in relation to the low logic level. Due to the slower characteristics of PZT-5H, when comparing the amplitude variations, the low logic level in OOK results still display a low amplitude level signal. Nonetheless, real tests (Figure 7a

and 7c) and simulation results (Figure 7b and 7d) show that information can still be recovered, but the signal displays a high level of degradation. Consequently, in adverse conditions such as turbulence, moving agents or by increasing the bitrate information, loss can occur.

In comparison, the PVDF transducers responses to BASK and OOK modulations are shown in Figure 8.

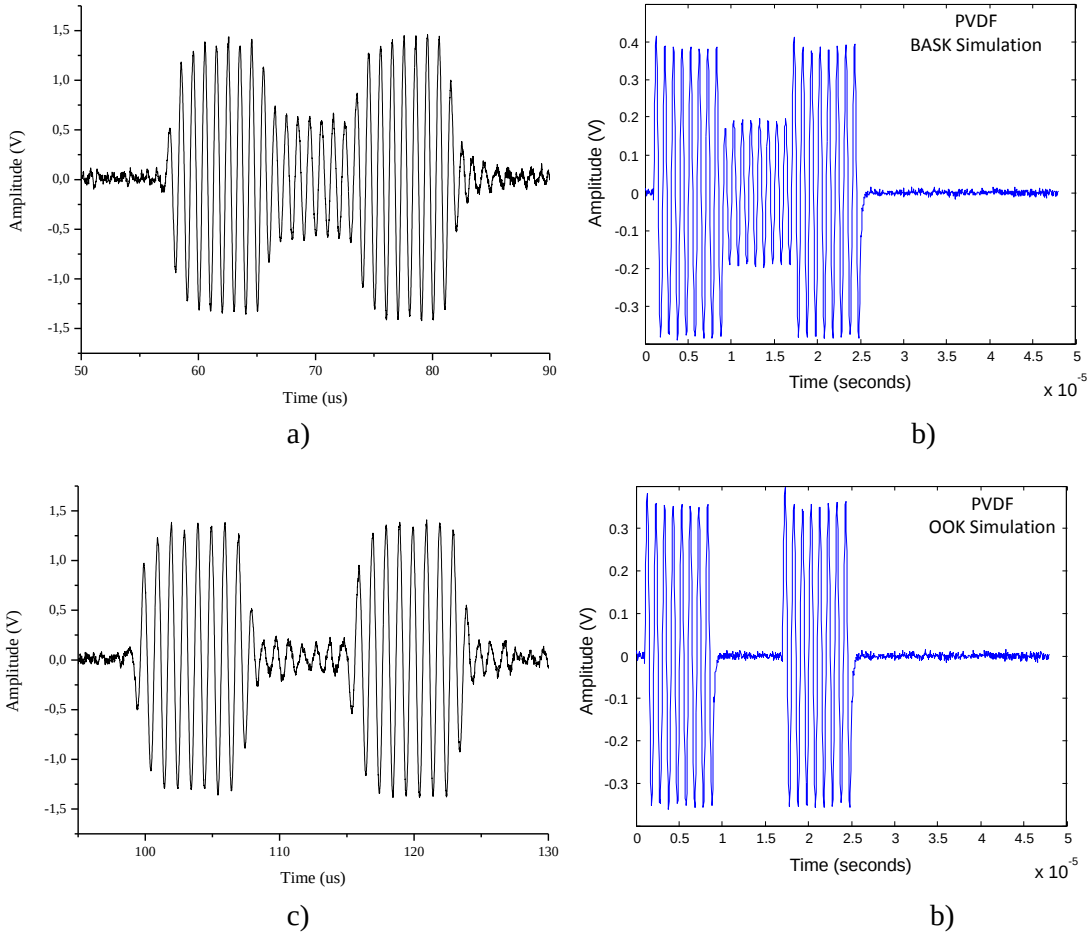

Figure 8: PVDF response to BASK and OOK modulation, real measurement and simulation.

Real tests (Figure 8a and 8c) are slightly slower in sudden amplitude transitions than in simulations (Figure 8b and 8d) for BASK and OOK modulations, and much of the signal deformations are due to echoes that overlap the signal. In fact, the remaining echoes that appear at the end of each signal (Figure 8c) imply that there is an intermediate signal. In general the signals show a high quality, resulting in easy information retrieval.

Figure 9 show the PZT-5H and PVDF transducers response to a BFSK modulation.

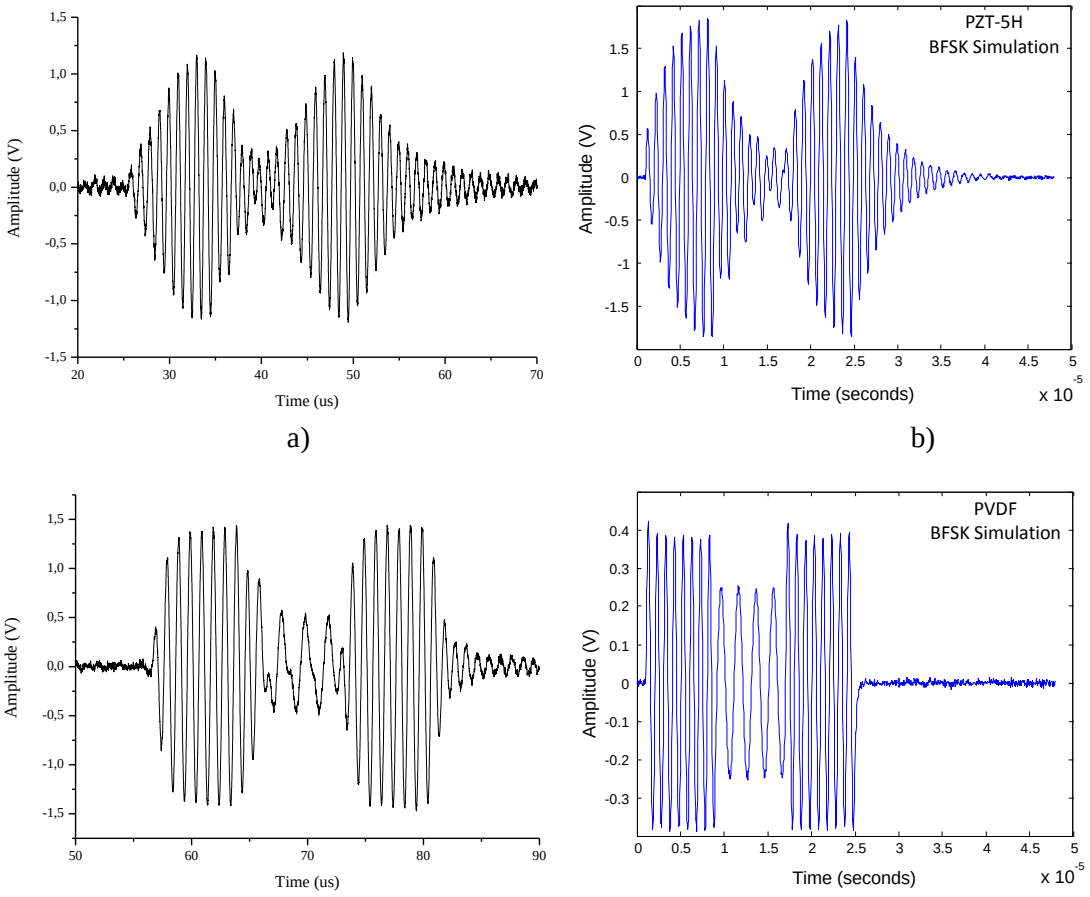

Figure 9: PZT-5H and PVDF response to BFSK modulation, real measurement and simulation.

Figures 9a and 9b show that the recovery of information in the 500 kHz signal is very difficult due to the high level of deformation. This is because the acoustic pressure is proportional to the frequency, resulting in a 500 kHz signal with half of the 1 MHz signal amplitude and also that the most of the acoustic pressure generated is retained inside the active material. This fact results in an overlapping of signals and a deformation on the 500 kHz signal. However, simulation results (Figure 9b) are shown to be very similar with the real tests (figure 9a), despite the remaining echoes that appeared in the real tests.

Figures 9c and 9d present the PVDF transducer response to the BFSK modulation. This signal shows a higher quality than the PZT-5H, where the small deformations, presented in real tests (Figure 9c), are due to the effect of remaining echoes.

Figure 10 shows the PZT-5H and PVDF transducers response to a BPSK modulation. BPSK was expected to be the worst of all the modulations due to their characteristics, since the stored energy has an opposite sign of the drive signal.

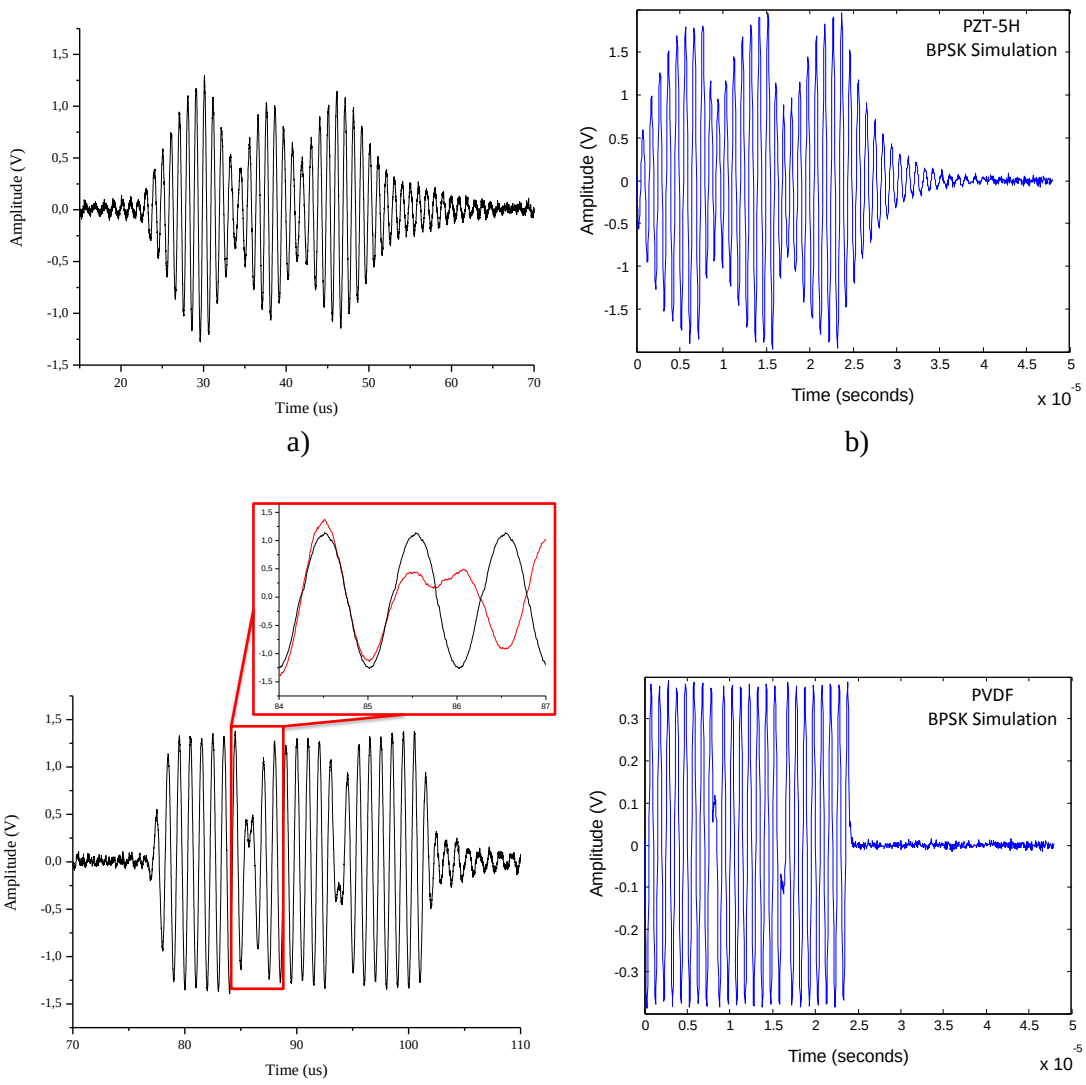

Figure 10: PZT-5H and PVDF response to BPSK modulation, real measurement and simulation.

As it is possible to observe in Figure 10a and 10b, the 180° phase shift is absorbed by the accumulated internal acoustic pressure, since both signals have opposite signs, masking the phase transition smoothly. But, in PVDF (Figure 10c), the case is sorely different.

For the PVDF real measurements (Figure 10c), the signal amplitude is highly reduced in the 180º phase shift. The main reason to this fact is that, when the 180° phase shift is applied, the resulting signal in the transducer has double the frequency with half amplitude and offset. The transducer tends therefore to produce an acoustic pressure with twice the frequency but without the necessary force. So it generates a stunted and deformed acoustic pressure wave. In simulation (Figure 10d) this effect is reduced, being an ideal model and without echoes. The signal is cleaner and therefore it will be easier to recover the information.

In a general way, PVDF shows better performance. Low acoustic impedance plays an important role in the non-periodic signals when using digital modulations. Real tests results are shown to be slightly slower in the sudden amplitude transitions than in the simulations results for all the modulations, and much of the signals deformations are due to echoes that overlap the signal, a fact which is ascribed to the reduced dimensions of the water tank.

5 Conclusions

A signal quality evaluation of ultrasonic transducers was carried out using Digital Modulations. Two types of transducers were tested: PZT-5H ceramic based transducers and PVDF polymers.

The study includes MATLAB/Simulink simulations and experimental validations for BASK, OOK, BFSK and BPSK modulations with a 1 MHz carrier at a 125 kbps baud rate.

Both materials show a non-linear acoustic output but, in a frequency range between 500 kHz and 1 MHz, PVDF shows an almost linear output with a 3.7 dB growth at 12 m. In contrast, PZT-5H shows a 19.6 dB growth.

It was concluded that PZT-5H resonance transducers are not suitable to be used with non-periodic high frequency signals. Signal deformation prevents a proper recovery of the information.

On the other hand, a PVDF transducer, with much lower acoustic impedance than PZT-5H, displays a better signal quality and, therefore, provides the signal full demodulation. On the other hand, the PZT-5H transducer has a higher output, but fails to perform accurate modulated signals.

Acknowledgment

This work was supported by FEDER through the COMPETE Program and by the Portuguese Foundation for Science and Technology (FCT) in the framework of the Strategic Project PEST-C/FIS/UI607/2011 and project PTDC/CTM-NAN/112574/2009. M. S. Martins thanks the FCT for the grant SFRH/BD/60713/2009.

References

Abrar, A, and S Cochran. 2004. "Multilayer Piezocomposite Structures with Piezoceramic Volume Fractions Determined by Mathematical Optimisation." *Ultrasonics* 42 (1-9): 259–65. doi:10.1016/j.ultras.2004.01.019.

Bove, Torsten, Wanda Wolny, Erling Ringgaard, and Annette Pedersen. 2001. "New Piezoceramic PZT–PNN Material for Medical Diagnostics Applications." *Journal of the European Ceramic Society* 21 (10-11): 1469–72. doi:10.1016/S0955-2219(01)00043-7.

Che, Xianhui, Ian Wells, Gordon Dickers, Paul Kear, and Xiaochun Gong. 2010. "Re-Evaluation of RF Electromagnetic Communication in Underwater Sensor Networks." *IEEE Communications Magazine* 48 (12): 143–51. doi:10.1109/MCOM.2010.5673085.

Chitre, Mandar, Shiraz Shahabudeen, and Milica Stojanovic. 2008. "Underwater Acoustic Communications and Networking: Recent Advances and Future Challenges." *Marine Technology Society Journal* 42 (1). IEEE: 103–16. doi:10.4031/002533208786861263.

EvoLogics. 2013. "EvoLogics GmbH." *Underwater Acoustic Modems*. http://www.evologics.de/en/products/acoustics/index.html.

Kim, Se-young, Jeong-woo Han, Ki-man Kim, Sang-hoon Baek, Hyung-chul Kim, and Chang-hwa Kim. 2010. "Experimental Results of Single Carrier Digital Modulation for Underwater Sensor Networks." *2010 IEEE/IFIP International Conference on Embedded and Ubiquitous Computing*, December. Ieee, 326–30. doi:10.1109/EUC.2010.54.

Leo, Donald J. 2007. *Engineering Analysis of Smart Material Systems*. John Wiley & Sons, Inc.

Levassort, F., L.P.Tran Huu Hue, G. Feuillard, and M. Lethiecq. 1998. “Characterisation of P(VDF-TrFE) Material Taking into Account Dielectric Relaxation: Application to Modelling of High Frequency Transducers.” *Ultrasonics* 36 (1-5): 41–45. doi:10.1016/S0041-624X(97)00081-4.

Lewin, P.A., and P.E. Bloomfield. 1997. “PVDF Transducers-a Performance Comparison of Single-Layer and Multilayer Structures.” *IEEE Transactions on Ultrasonics, Ferroelectrics and Frequency Control* 44 (5): 1148–56. doi:10.1109/58.655640.

Martins, M, V Correia, J.M. Cabral, S Lanceros-Mendez, and J.G. Rocha. 2012. “Optimization of Piezoelectric Ultrasound Emitter Transducers for Underwater Communications.” *Sensors and Actuators A: Physical* 184 (September). Elsevier B.V. 141–48. doi:10.1016/j.sna.2012.06.008.

Martins, M.S., V Correia, S. Lanceros-Mendez, J.M. Cabral, and J.G. Rocha. 2010. “Comparative Finite Element Analyses of Piezoelectric Ceramics and Polymers at High Frequency for Underwater Wireless Communications.” *Procedia Engineering* 5 (January): 99–102. doi:10.1016/j.proeng.2010.09.057.

Martins, M.S., N. Pinto, G. Rocha, J. Cabral, and S. Laceros Mendez. 2014. “Development of a 1 Mbps Low Power Acoustic Modem for Underwater Communications.” In *2014 IEEE International Ultrasonics Symposium*, 2482–85. IEEE. doi:10.1109/ULTSYM.2014.0619.

Nowsheen, Nusrat, Craig Benson, and Michael Frater. 2010. “A High Data-Rate, Software-Defined Underwater Acoustic Modem.” In *OCEANS 2010 MTS/IEEE SEATTLE*, 1–5. IEEE. doi:10.1109/OCEANS.2010.5664474.

Preisig, James. 2006. “Acoustic Propagation Considerations for Underwater Acoustic Communications Network Development.” In *Proceedings of the 1st ACM International Workshop on Underwater Networks - WUWNet ’06*, 11:1. New York, New York, USA: ACM Press. doi:10.1145/1161039.1161041.

Saitoh, S, T Kobayashi, K Harada, S Shimanuki, and Y Yamashita. 1998. “A 20 MHz Single-Element Ultrasonic Probe Using 0.91Pb(Zn(1/3)Nb(2/3))O(3)-0.09PbTiO(3) Single Crystal.” *IEEE Transactions on Ultrasonics, Ferroelectrics, and Frequency Control* 45 (4): 1071–76. doi:10.1109/58.710590.

Sameer, Babu.T.P, R. David Koilpillai, and P. Muralikrishna. 2012. “Underwater Acoustic Communications: Design Considerations at the Physical Layer Based on Field Trials.” *2012 National Conference on Communications (NCC)*, February. Ieee, 1–5. doi:10.1109/NCC.2012.6176782.

Schmerr, L W, a Lopez-Sanchez, and R Huang. 2006. “Complete Ultrasonic Transducer Characterization and Its Use for Models and Measurements.” *Ultrasonics* 44 Suppl 1 (December): e753–7. doi:10.1016/j.ultras.2006.05.088.

Sencadas, V., R. Gregorio, and S. Lanceros-Mendez. 2009. “A to B Phase Transformation and Microestructural Changes of PVDF Films Induced by Uniaxial Stretch.” *Journal of Macromolecular Science, Part B* 48 (3): 514–25. doi:10.1080/00222340902837527.

Sherman, Charles H., and John L. Butler. 2007. *Transducers and Arrays for Underwater Sound*. Springer Science+Business Media, LLC.

Shrout, Thomas R. 2008. “Innovations in Piezoelectric Materials for Ultrasound Transducers.” In *2008 17th IEEE International Symposium on the Applications of Ferroelectrics*, 1–4. IEEE. doi:10.1109/ISAF.2008.4693822.

Stojanovic, Milica, and James Preisig. 2009. “Underwater Acoustic Communication Channels: Propagation Models and Statistical Characterization.” *IEEE Communications Magazine* 47 (1): 84–89. doi:10.1109/MCOM.2009.4752682.

Wang, Yi-Chun, Ching-Hung Huang, Yung-Chun Lee, and Ho-Hsun Tsai. 2006. “Development of a PVDF Sensor Array for Measurement of the Impulsive Pressure Generated by Cavitation Bubble Collapse.” *Experiments in Fluids* 41 (3): 365–73. doi:10.1007/s00348-006-0135-8.

Yamamoto, Noriko, Yohachi Yamashita, Yasuharu Hosono, and Kazuhiro Itsumi. 2013. “Electrical and Physical Properties of Repoled PMN–PT Single-Crystal Sliver Transducer.” *Sensors and Actuators A: Physical* 200 (October): 16–20. doi:10.1016/j.sna.2012.10.002.